J. Eur. Opt. Society-Rapid Publ. 2022, **18**, 13

https://doi.org/10.1051/jeos/2022013
Available online at: jeos.edpsciences.org

**Journal of the European Optical Society-Rapid Publications**

**EOSAM 2021**
Guest editors: Concita Sibilia, Alessandro Belardini and Gilles Pauliat

RESEARCH ARTICLE OPEN ACCESS

# Terahertz spectra of electrolyte solutions under applied electric and magnetic fields

Yan Shen[1,2,3,4], Qingjun Li[1,2,3,4], Jing Ding[1,2,3,4], Guoyang Wang[1,2,3,4], Fengxuan Zhang[4], Bo Su[1,2,3,4,*], and Cunlin Zhang[1,2,3,4]

[1] Key Laboratory of Terahertz Optoelectronics, Ministry of Education, Beijing 100048, China
[2] Beijing Key Laboratory of Terahertz Spectroscopy and Imaging, Beijing 100048, China
[3] Beijing Advanced Innovation Center for Imaging Theory and Technology, Beijing 100048, China
[4] Department of Physics, Capital Normal University, Beijing 100048, China

Received 18 November 2021 / Accepted 22 November 2022

**Abstract.** Most biomolecules require an aqueous environment to fully exert their biological activity. However, the rotation mode, vibration mode, and energy associated with the hydrogen bonding network of water are in the terahertz band, resulting in strong absorption. Therefore, it is difficult to detect liquid biological samples using the terahertz technology. Here, a high-transmittance double-layer microfluidic chip was prepared using a cycloolefin copolymer material with high transmittance of terahertz waves. Combined with terahertz time-domain spectroscopy, the terahertz spectral characteristics of deionized water, NaCl, $NaCO_3$, and $CH_3COONa$ solutions were studied. The changes in the terahertz transmission intensity of these electrolyte solutions under constant electric and magnetic fields were measured. The results show that the terahertz spectra of different sodium salt solutions with the same concentration of 0.9 mol/L are different. Furthermore, the terahertz absorption coefficients of the different electrolyte solutions gradually decrease with the increase of their residence time under the electric field, which is contrary to the results obtained under the external magnetic field. This study provides a new idea for the detection of sodium salt solution and lays a foundation for the development of THz technology.

**Keywords:** Terahertz, Microfluidic chip, Electric field, Magnetic field, Sodium salt solution.

### Abbreviations

| | |
|---|---|
| PBS | Polarisation Beam Splitter; |
| PCA | Photoconductive Antenna; |
| THz | Terahertz; |
| THz-TDS | THz Time Domain Spectroscopy. |

## 1 Introduction

The terahertz (THz) wave is located between the microwave and infrared regions of the electromagnetic spectrum [1], in the frequency range of 0.1–10 THz. The THz technology offers a new route for detecting biomolecules. Since the vibration and rotation energy levels of many biomolecules are in the THz band and the energy is distributed between electrons and photons, harmless to substances [2], the THz technology can be utilized to detect biomolecules. In addition, since many biomolecules require an aqueous solution to exert their biological activity, it is necessary to study the characteristics of biological samples in aqueous solutions [3]. However, the internal hydrogen bonding network of aqueous solutions induces the strong absorption of THz waves, which significantly hinders the detection of the THz signal [4]. By combining the THz technology with microfluidic technology, the absorption of THz waves by liquid samples can be significantly reduced, enabling the detection of THz signals with high accuracy. Liu et al. [5] combined transmission THz frequency-domain spectroscopy with a quartz-based microcrystalline subsystem, which achieved good transmission performance in the preliminary detection of an isopropanol water mixture in the frequency range of 0.570–0.630 THz. Wu et al. [6] combined THz technology with a sandwich microfluidic chip, studied the THz characteristics of different concentrations of KCl, KBr, $MgCl_2$ and $CaCl_2$ in the frequency range of 0.1–1 THz, and found that some electrolytes promote the formation of hydrogen bonds, while others promote the breaking of hydrogen bonds. Tang et al. [7] proposed a

* Corresponding author: su-b@163.com

simple and inexpensive cell-capture microfluidic chip prototype for the THz spectral research of living cells. However, in their experiments, they did not combine the liquid solutions with electromagnetic fields to further explore the THz characteristics of these solutions.

With a decrease in the supply of biological samples for biological detection, particularly expensive biological reagents or environmentally unfriendly biological samples, the sample size used in experiments has gradually decreased from liters and milliliters to microliters, nanoliter, and even picoliters. This development gave rise to microfluidic technology, which involves using microchannels to control very small liquid volumes. Microfluidic technology has the advantages of small volume requirement (manipulation of nano amounts), low cost, and fast detection [8]. Zhang et al. [4] used a newly developed microfluidic chip as an effective sensor to detect the THz absorption characteristics of microcystin aptamers dissolved in different concentrations of aminobutanol and trimethylolaminomethane buffer. Alfihed et al. [9] utilized two low-cost polymers as potential THz microfluidic chip materials, one made of phthalate and the other made of ultrahigh molecular weight polyethylene, to measure the absorption spectrum of silicone rubber curing agent. Liu et al. [10] used an SU-8 photoresist to fabricate an ultrathick microfluidic chip for THz spectrum detection, and they used the chip to detect the absorption coefficient in the frequency range of 0.1–1.5 THz. The THz transmittance of the microfluidic chip could only reach a generally high level. At present, the widely used microfluidic system conventionally adopts silicon, glass, or polymer polydimethylsiloxane (PDMS). For biological samples or liquid samples in water, silicon is relatively expensive and opaque to visible light. Therefore, it is not suitable for application because it is impossible to directly observe whether the microfluidic chip is filled with the liquid sample. The THz absorption of ordinary glass is quite strong; thus, the THz transmittance of a glass-based microfluidic chip is considerably low, and it is not suitable for the fabrication of the THz microfluidic chip. The optical properties of the cyclic olefin copolymer (COC) used in this experiment are comparable to those of polymethylmethacrylate (PMMA), and its heat resistance is higher than that of polycarbonate (PC). In addition, it exhibits almost no water absorption, better dimensional stability than those of PMMA and PC, and high THz transmittance. In addition, COC has the advantages of decreasing water–vapor permeability and increasing rigidity; it also exhibits good heat resistance and can be easily cut. Thus, it is the best alternative to glass materials, and it fundamentally enables the control of the molecular concentration in time and space.

In this study, a THz microfluidic chip is bonded using an acrylic adhesive. Compared with resin and PDMS, COC materials exhibit high transmittance in the THz range. Different sodium salt electrolyte solutions with the same concentration are prepared, and their THz transmission characteristics are studied using a microfluidic chip combined with THz time-domain spectroscopy (THz-TDS). It is found that the addition of electrolyte will destroy the hydrogen bond network in the solution, thereby altering the THz transmission spectrum. In addition, we further explored the THz transmission characteristics of electrolyte solution in magnetic field and electric field for different time. The results show that the THz transmission intensity of different electrolyte solutions under electric field increases gradually with the increase of residence time, but the results are opposite under external magnetic field. This indicates that the hydrogen bond in electrolyte solution will be affected by external electric field or magnetic field, and the degree will increase or decrease with the extension of residence time.

## 2 Experiment

### 2.1 Fabrication of the microfluidic chip

We employed COC to fabricate the THz microfluidic chips. The THz transmittance of this material could reach more than 95%, and there is no noticeable absorption peak. In addition, COC is transparent in the visible light region and is very suitable for studying the THz characteristics of biological samples.

Firstly, the COC material (thickness: 2 mm; length and width: 20 mm × 20 mm) was milled using the Computer Numerical Control milling machine to mill the liquid pool in the detection area with a length of 15 mm, width of 10 mm, and depth of 0.1 mm, as well as the liquid inlet channel, liquid outlet channel, and square transition zone on the left and right sides. Thereafter, a COC material of the same size was selected as the cover. Secondly, a 1 mm-diameter drill bit was used to drill holes on the side surface of the substrate and connect to the square transition zone. Finally, the cover sheet of the COC material was bonded to the milled substrate using an acrylic adhesive, and the liquid inlet and outlet channels in the COC material were connected to the liquid pool through the transition zone. The preparation process of the microfluidic chip is shown in Figure 1.

### 2.2 Experimental system

The optical path of the experimental system is shown in Figure 2, which is mainly composed of femtosecond laser, THz radiation generation device, corresponding detection device and time delay control system. The system uses a self-mode-locked fiber femtosecond laser independently developed and customized by Peking University (the center wavelength is 1550 nm, the pulse width is 75 fs, the pulse repetition frequency is 100 MHz, and the output power is 130 mW). The laser passing through the beam splitter is divided into pump pulse and detection pulse. The former is coupled into the optical fiber photoconductive antenna (*BATOP Company* bpca-100-05-10-1550-c-f) through the time delay system to excite and generate THz pulses, and the latter is coupled into the optical fiber photoconductive antenna (*BATOP Company* bpca-180-05-10-1550-c-f) to detect THz wave. The microfluidic chip is fixed between two off-axis parabolic mirrors. When the THz wave generated passes through the chip, it carries the sample information, which is amplified by the phase-locked amplifier and transmitted to the computer. Finally, the computer collects and processes the data.

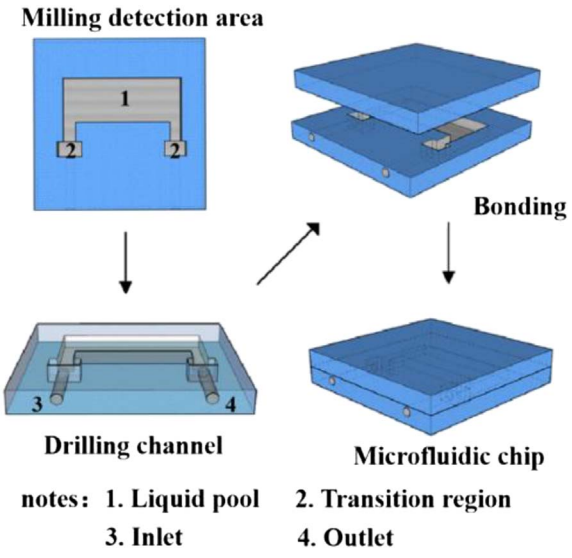


**Fig. 1.** Preparation flow chart of the THz microfluidic chips.

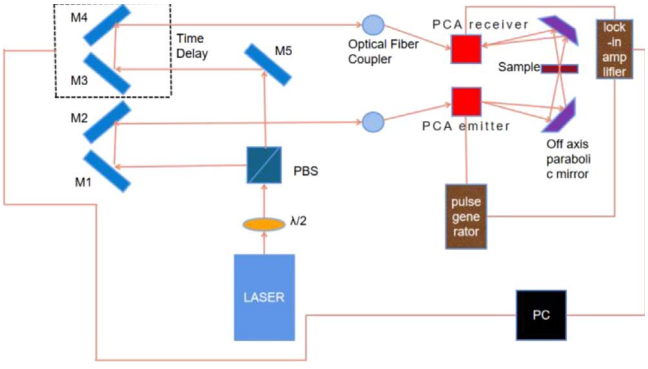


**Fig. 2.** Optical path diagram of experimental system.

## 2.3 Experimental device for applying the external high-voltage electric field

The schematic diagram of the experimental device employed to apply the electric field in this experiment is shown in Figure 3. The experimental device includes a high-voltage power module, sliding rheostat, 0–5 V switching power supply connected to the sliding rheostat, 0–10,000 V output high-voltage power module, and 12 V switching power supply. The 5 V switching power supply and sliding rheostat form a voltage dividing circuit to adjust the output of the high-voltage power module. The 12 V switching power supply supplies power to the high-voltage module, and the output end of the high-voltage power module is respectively connected to two opposite metal plates with wires. To ensure that the electric field of the microfluidic chip is uniform, the size of the two metal sheets was set as 8 cm × 15 cm, which is larger than the size structure of the microfluidic chip. The microfluidic chip was placed in the middle of the two metal plates; the spacing between the two metal plates was 4 cm, and the field strength between the plates was 2500 V/cm.

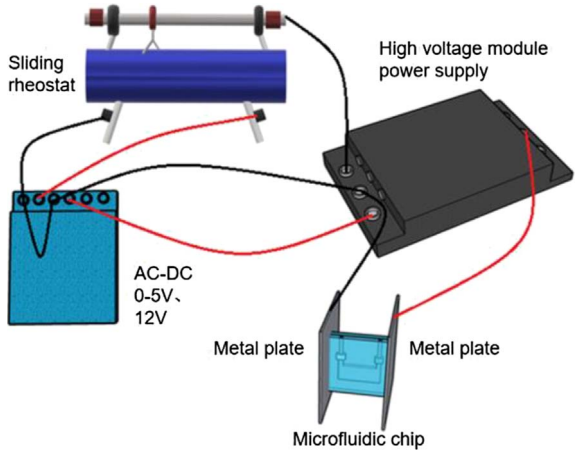


**Fig. 3.** Schematic diagram of the experimental device for applying the external electric field.

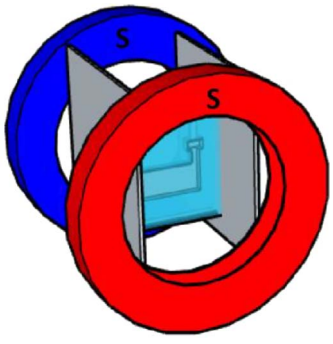


**Fig. 4.** Schematic diagram of the experimental device for applying the external magnetic field.

## 2.4 Experimental device for applying the external magnetic field

The schematic diagram of the experimental device used to apply external magnetic field in this experiment is shown in Figure 4. The microfluidic chip is placed on the position where the N-pole and S-pole of the electromagnet are parallel and symmetrical. The magnetic field generated at this position is a uniform magnetic field with a magnetic field strength of 88 mT.

## 2.5 Experimental process

In the experiments, we explored the destructive effect of the electrolytes on the hydrogen bonds between the water molecules. Firstly, NaCl, $Na_2CO_3$, and $CH_3COONa$ solutions with a molar concentration of 0.9 mol/L were investigated. This concentration was adopted because $Na_2CO_3$ reaches saturation when the concentration is higher than 0.9 mol/L. These electrolyte solutions have the same cation, namely $Na^+$, which is a very important electrolyte in the human body. It is essential in maintaining human physiological metabolism and normal function. Adults ingest approximately 5–8 g of $Na^+$ daily, and the intestinal tract

secretes approximately 30 g of $Na^+$. Sodium salt solutions are non-toxic and harmless to the human body, and the sample preparation process is safe. Therefore, the use of the sodium salt solution as the test sample in this study is highly beneficial. Deionized water and the above sodium salts were successively injected into the microfluidic chip, after which the self-built THz-TDS system was employed for the detection. Firstly, the THz-TDS spectra were obtained; thereafter, the corresponding frequency-domain spectra were obtained by Fourier transform. The spectral information of each solution was compared with that of deionized water. The experimental results are shown in Figure 5. By observing the spectral intensity of each electrolyte, it was found that the spectral intensities of these three electrolytes are lower than that of deionized water. Since the absorption of THz by water is mainly due to the hydrogen bonding network in the water, it can be judged that the three electrolytes promote the formation of hydrogen bonds between water molecules to varying degrees, thus reducing the intensity of the THz spectra. The order of the hydrogen bonding promotion degree is $CH_3COONa > Na_2CO_3 > NaCl$.

Secondly, the THz transmission characteristics of the NaCl, $Na_2CO_3$, and $CH_3COONa$ solutions with the same concentration at different time under the electric field were studied using the THz-TDS system. The experimental results are shown in Figures 6–8. In each figure, (a) shows the THz frequency domain spectra, (b) shows the absorption coefficient and (c) shows the change curve of absorption coefficient with time at the frequency value when the spectrum reaches the maximum (i.e. about 0.15 THz). The absorption coefficient is obtained according to formula (1), where $c$ is the solution concentration, $d$ is the thickness of the liquid pool, $R$ is the amplitude value after Fourier transform when scanning a single blank film, $S$ is the amplitude value and $A$ is the absorption coefficient.

$$A = \frac{1}{cd} \ln \frac{R}{S}. \quad (1)$$

It can be observed that the spectra of NaCl, $Na_2CO_3$, and $CH_3COONa$ increase with the increase of residence time after electric field treatment, and the order is 20 min > 15 min > 10 min > 5 min > 0 min. On the contrary, the absorption coefficient decreases with the increase of residence time under the applied electric field. This indicates that the hydrogen bond in electrolyte solution will be destroyed under the action of external electric field, and the degree of destruction will increase with the extension of residence time.

Next, the microfluidic chip filled with 0.9 mol/L NaCl, $Na_2CO_3$, and $CH_3COONa$ solutions was placed under a uniform magnetic field for different time, after which the THz transmission characteristics were studied. The residence time were 0, 5, 10, 15, and 20 min. The experimental results are shown in Figures 9–11. Similar to the situation in electric field, (a), (b) and (c) in each figure are THz frequency domain spectra, absorption coefficient diagram and change curve of absorption coefficient with time at the frequency value when the spectrum reaches the maximum (i.e. about 0.17 THz). It can be observed that the

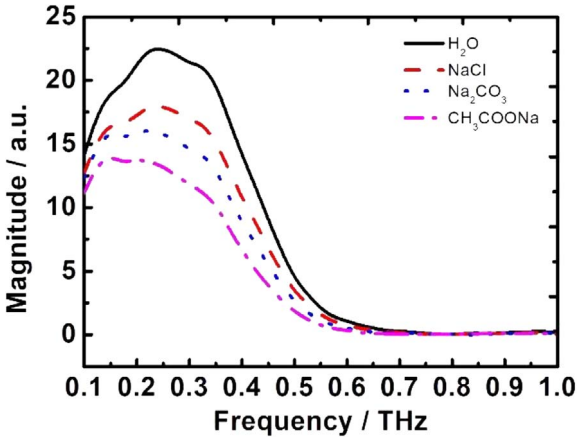


**Fig. 5.** Spectra of the 0.9 mol/L NaCl, $Na_2CO_3$, and $CH_3COONa$ solutions.

THz frequency domain spectra of NaCl, $Na_2CO_3$, and $CH_3COONa$ solutions exposed to the magnetic field decrease with the increase of residence time, in the order of 0 min > 5 min > 10 min > 15 min > 20 min. On the contrary, the absorption coefficient increases with the increase of residence time under the applied magnetic field. This indicates that the number of hydrogen bonds in the electrolyte solution will gradually increase under the external magnetic field, which is contrary to the results observed under the electric field.

## 3 Results and discussion

Water is the most important liquid in biological media. The basic objective of chemistry and biology is to understand the molecular structure of liquid water, particularly the hydrogen bond between water molecules [11]. The biochemical interaction between liquid water and biomolecules constitutes the biological environment and influences the activity of the biomolecules. The intramolecular and intermolecular dynamics of biomolecules influence the hydrogen bonds between water and biomolecules or between water molecules themselves. The typical time scale of the water hydrogen-bond network at room temperature is in the picosecond range, and the corresponding frequency is several THz. For decades, the THz spectrum has been utilized to explain the dielectric relaxation, hydrogen bonding network, and ultrafast dynamics of liquids, including water and molecules, as well as polar/nonpolar liquids. The energy of the hydrogen bond of water is 2.6 kJ/mol, which is less than that of a covalent bond or ionic bond, but greater than van der Waals force. Both water and biomolecules (such as DNA and protein) contain hydrogen bonds. A water molecule contains two electronegative soliton pairs, owing to the presence of oxygen. Each soliton pair can form hydrogen bonds with other water molecules, as shown in Figure 12. The hydrogen bonds between molecules account for the different phases of water, such as liquid and solid phases. When the three solutes are dissolved in

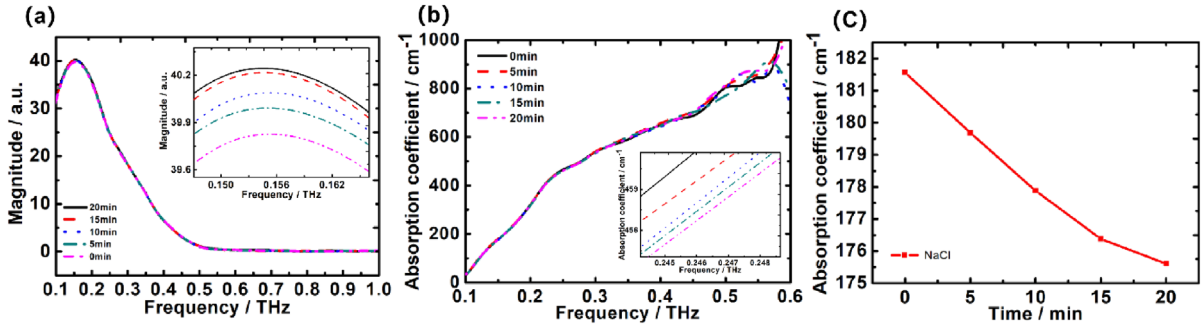


**Fig. 6.** THz spectra of NaCl solution under an applied electric field at different time. (a) THz frequency domain spectra, (b) absorption coefficient and (c) relationship between absorption coefficient and residence time at the selected frequency of 0.15 THz.

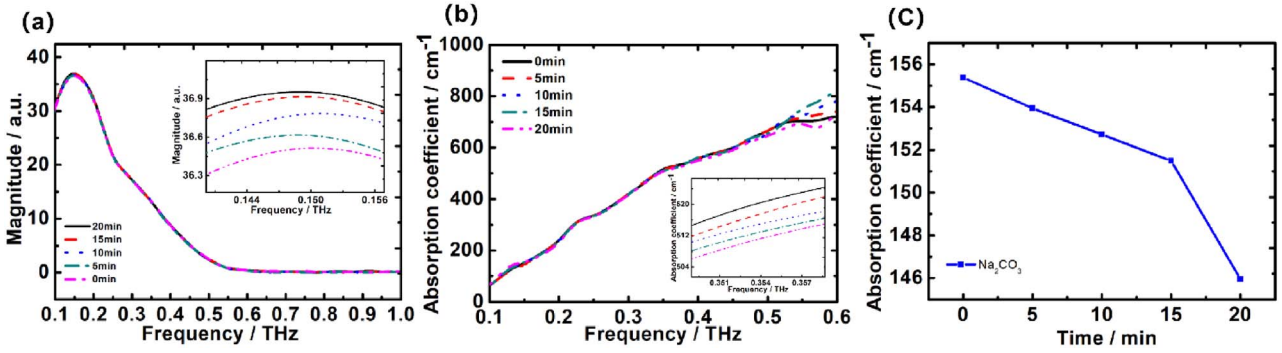


**Fig. 7.** THz spectra of $Na_2CO_3$ solution under an applied electric field at different time. (a) THz frequency domain spectra, (b) absorption coefficient and (c) relationship between absorption coefficient and residence time at the selected frequency of 0.15 THz.

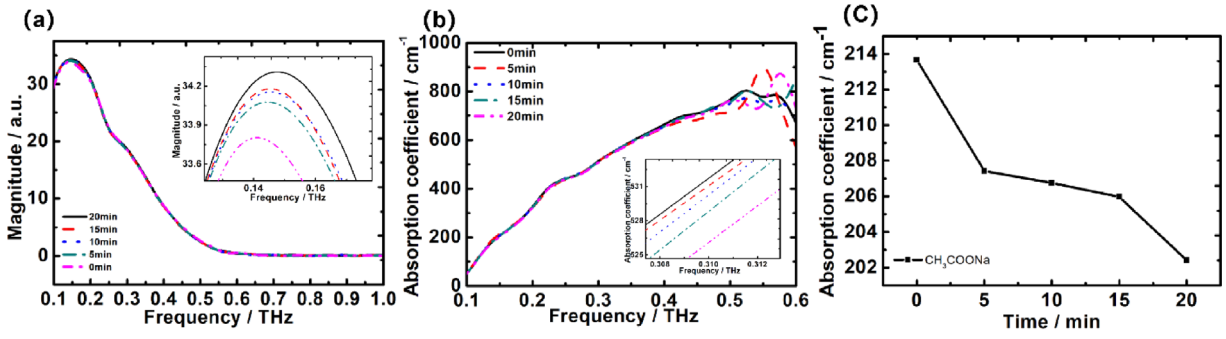


**Fig. 8.** THz spectra of $CH_3COONa$ solution under an applied electric field at different time. (a) THz frequency domain spectra, (b) absorption coefficient and (c) relationship between absorption coefficient and residence time at the selected frequency of 0.15 THz.

water, the electric field formed near the ions will rearrange the solvent water molecules around the ions. The electric field intensity on the surface of monovalent metal ions with a radius of 200–300 pm is approximately 108 V $cm^{-1}$ [12]. Such a high electric field intensity is sufficient to rearrange the dipole water molecules near the ions, change the microstructure of the water in the ion hydration layer, and increase the number of hydrogen bonds between the water molecules; moreover, different electrolyte solutions have different increment effects on the number of hydrogen bonds. Therefore, the THz transmission intensity of the electrolyte solutions is less than that of water and varies with the electrolyte.

In this study, the THz frequency-domain spectral information of the three sodium salt solutions at the same concentration was measured, and the three solutions were exposed to electric and magnetic fields at different time. Water molecules are polar, and there is an electric dipole interaction between them. Under an applied electric field, water molecules will undergo polarization, and the direction

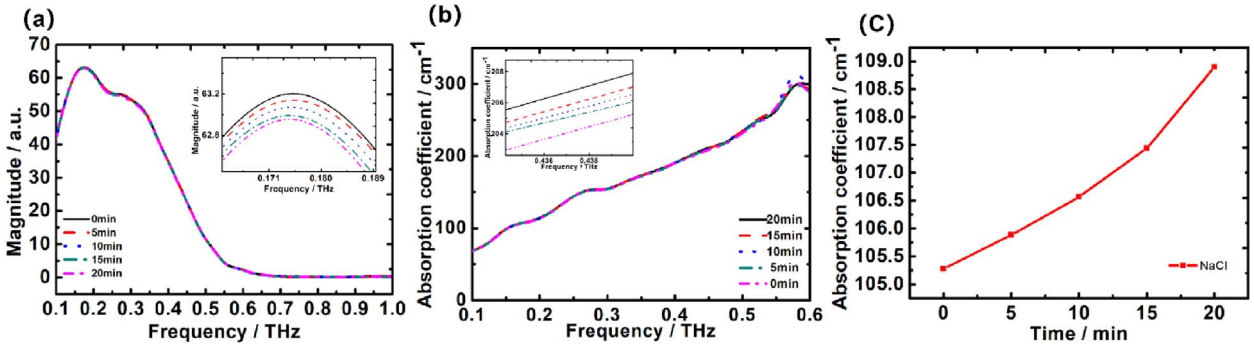


**Fig. 9.** THz spectra of NaCl solution under an applied magnetic field at different time. (a) THz frequency domain spectra, (b) absorption coefficient and (c) relationship between absorption coefficient and residence time at the selected frequency of 0.17 THz.

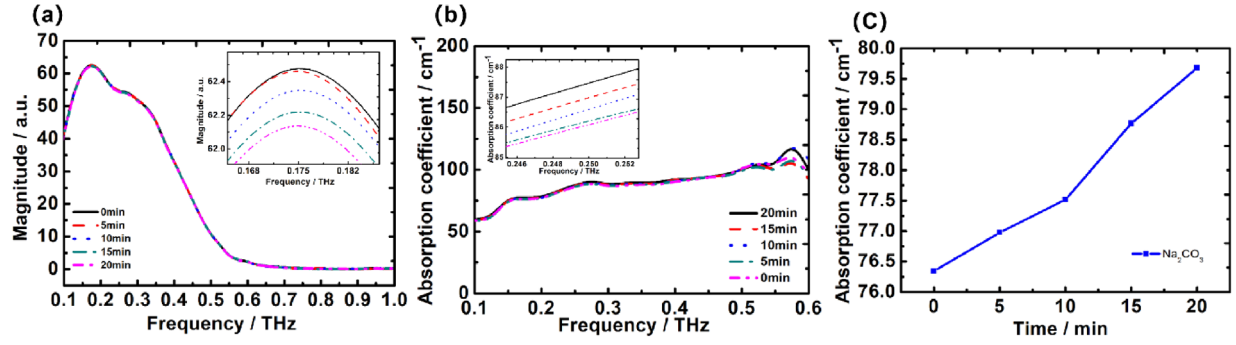


**Fig. 10.** THz spectra of $Na_2CO_3$ solution under an applied magnetic field at different time. (a) THz frequency domain spectra, (b) absorption coefficient and (c) relationship between absorption coefficient and residence time at the selected frequency of 0.17 THz.

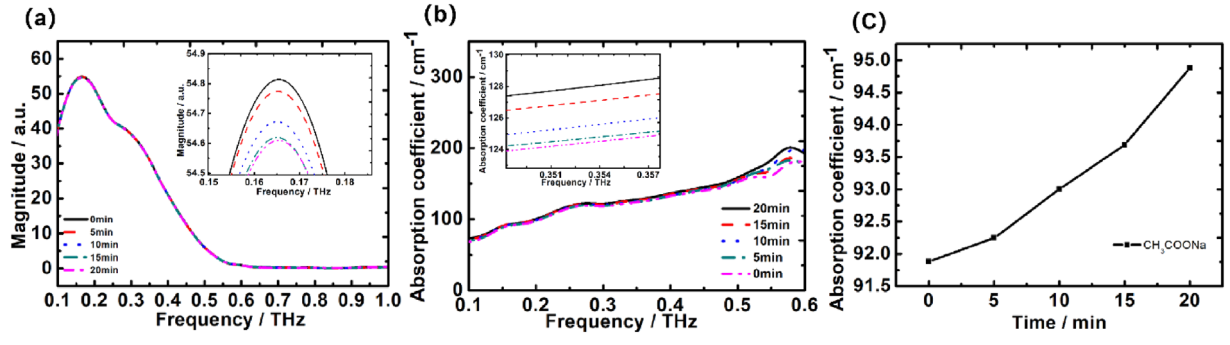


**Fig. 11.** THz spectra of $CH_3COONa$ solution under an applied magnetic field at different time. (a) THz frequency domain spectra, (b) absorption coefficient and (c) relationship between absorption coefficient and residence time at the selected frequency of 0.17 THz.

of the dipole moment will change along the direction of the applied electric field. When the applied electric field strength changes, the rotation angle of the dipole moment also changes. Due to the change in the dipole moment angle in water molecules, the external electric field treatment of the electrolyte solution will affect the vibration, rotation, and spatial structure of all the water molecules [13]. Many scholars have repeatedly studied magnetized water exposed to a magnetic field, and they have found that many of the physical properties of water change under the magnetic field, such as the pH, surface tension, osmotic pressure, viscosity coefficient, and dielectric constant. Chang and Weng [14]. simulated the effect of an external magnetic field on the number of hydrogen bonds in solution by molecular dynamics. They found that magnetic fields stabilize the structure of water and promote the formation of hydrogen bonds between water molecules, which is consistent with our experimental results.

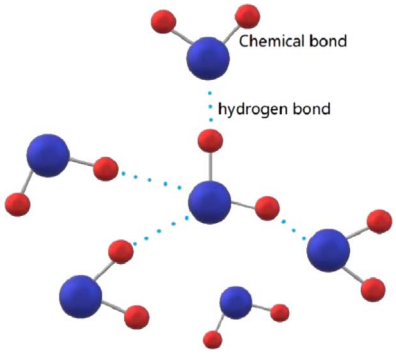


**Fig. 12.** Schematic diagram of the hydrogen bonding among water molecules.

## 4 Conclusion

In this study, THz technology and microfluidic technology were combined to study the spectral characteristics of NaCl, $Na_2CO_3$ and $CH_3COONa$ electrolyte solutions with a concentration of 0.9 mol/L, the THz spectral intensity and absorption coefficient at different time in electric and magnetic fields and the relationship between absorption coefficient and standing time at fixed frequency. Firstly, deionized water and NaCl, $Na_2CO_3$, and $CH_3COONa$ solutions of the same concentration were investigated. The results showed that when the cation is $Na^+$, the order of the THz spectral intensity is NaCl > $Na_2CO_3$ > $CH_3COONa$, indicating that the three electrolyte solutions promote the association of hydrogen bonds between water molecules in different degrees. Subsequently, the solutions were placed under electric and magnetic fields for different time. It was observed that the THz transmission intensity increases and the absorption coefficient decreases as the residence time of the solution increases, indicating that the hydrogen bond in the electrolyte solution will be destroyed by the applied electric field, and the destruction magnitude will increase with the residence time. The THz transmission intensity in the magnetic field is opposite to that in the electric field. The results show that the transmission intensity of THz decreases and the absorption coefficient increases with the increase of the residence time of the solution in the magnetic field, indicating that the number of hydrogen bonds in the electrolyte solution will gradually increase. The experimental results provides technical support for exploring the micro field to study the dynamic characteristics of molecules.

*Acknowledgments.* We would like to thank Editage (https://www.editage.com) for English language editing.

## Authors' Contributions

Yan Shen is the main author of this manuscript. Bo Su is the corresponding author of this manuscript. All authors contributed to the theoretical analysis, calculations, experiment, and preparation of the manuscript.

## Funding

This work was supported by the National Natural Science Foundation of China under grant number 61575131.

## Availability of data and materials

Information about data was detailed in the article.

## Declarations

### Ethics approval and consent to participate

Ethics approval and consent to participate were not required.

### Consent for publication

Consent for publication is not applicable.

## Conflicts of interest

The authors declare that they have no conflicts of interest.

## References

1 Vafapour Z., Keshavarz A., Ghahraloud H. (2020) The potential of terahertz sensing for cancer diagnosis, *Heliyon* **6**, e05623.
2 Wen Y., Su B., Wang J., Wang G., Wu Y., He J., Zhang C. (2020) Terahertz spectral analysis of different electrolytes, *Opt. Eng.* **59**, 055107.
3 Hou L., Shi W., Dong C., Yang L., Wang Y., Wang H., Hang Y., Xue F. (2020) Probing trace lactose from aqueous solutions by terahertz time-domain spectroscopy, *Spectrochim. Acta A Mol. Biomol. Spectrosc.* **246**, 119044.
4 Zhang M., Yang Z., Tang M., Wang D., Wang H., Yan S., Wei D., Cui H. (2019) Terahertz spectroscopic signatures of microcystin aptamer solution probed with a microfllfluidic chip, *Sensors* **19**, 534.
5 Lei L., Pathak R., Cheng L., Wang T. (2013) Real-time frequency-domain terahertz sensing and imaging of isopropyl alcohol–water mixtures on a microfluidic chip – ScienceDirect, *Sens. Actuators B: Chem* **184**, 228–234.
6 Wu Y., Su B., He J., Zhang C. (2019) Terahertz absorption characteristics of electrolyte solution based on microfluidic chip, *Spectrosc. Spect. Anal.* **39**, 2348–2353.
7 Tang Q., Liang M., Lu Y., Wong P., Wilmink G., Zhang D., Xin H. (2016) Microfllfluidic devices for terahertz spectroscopy of live cells toward lab-on-a-chip applications, *Sensors* **16**, 476.
8 Dai L., Zhao X., Guo J., Feng S., Fu Y., Kang Y., Guo J. (2020) Microfllfluidics-based microwave sensor, *Sens. Actuator. A Phys.* **309**, 111910.
9 Alfihed S., Bergen M.H., Holzman J.F., Foulds I.G. (2018) Fabrication of low-cost microfluidic chip for terahertz detection applications, *IEEE 13th Annual International Conference on Nano/Micro Engineered and Molecular Systems (NEMS)*, pp. 52–55, https://doi.org/10.1109/NEMS.2018.8557013.

10 Liu M., Zhou D., Zhang M., Cui H.-L., Wang D. (2016) A microfluidic chip for terahertz spectral detection, in: *IEEE International Conference on Manipulation, Manufacturing and Measurement on the Nanoscale (3M-NANO)*, pp. 59–63. https://doi.org/10.1109/3M-NANO.2016.7824965.
11 De Ninno A., Nikollari E., Missori M., Frezza F. (2020) Dielectric permittivity of aqueous solutions of electrolytes probed by THz time-domain and FTIR spectroscopy, *Phys. Lett.* **384**, 126865.
12 Wang W., Zhao L., Yan B. (2010) Effects of ions on structure of liquid water, *Chem. Bull.* **73**, 06, 491–498. https://doi.org/10.14159/j.cnki.0441-3776.2010.06.001.
13 Hajime T. (2015) *International Conference of Computational Methods in Sciences and Engineering*, American Institute of Physics, p. 090043.
14 Chang K., Weng C. (2006) The effect of an external magnetic field on the structure of liquid water using molecular dynamics simulation, *J. Appl. Phys.* **100**, 2923.